

ห้องสมุดงานวิจัย สำนักงานคณะกรรมการการวิจัยแห่งชาติ



E47207

**SYNTHESIS AND CHARACTERIZATION OF METAL TELLURIDES AND
ANTIMONIDES FOR USING AS THERMOELECTRIC MATERIALS**

TAWAT SURIWONG

**DOCTOR OF PHILOSOPHY
IN MATERIALS SCIENCE**

**THE GRADUATE SCHOOL
CHIANG MAI UNIVERSITY
APRIL 2011**

60052901

ห้องสมุดงานวิจัย สำนักงานคณะกรรมการวิจัยแห่งชาติ



E47207

**SYNTHESIS AND CHARACTERIZATION OF METAL TELLURIDES AND
ANTIMONIDES FOR USING AS THERMOELECTRIC MATERIALS**



TAWAT SURIWONG

**A THESIS SUBMITTED TO THE GRADUATE SCHOOL IN
PARTIAL FULFILLMENT OF THE REQUIREMENTS
FOR THE DEGREE OF
DOCTOR OF PHILOSOPHY
IN MATERIALS SCIENCE**

**THE GRADUATE SCHOOL
CHIANG MAI UNIVERSITY
APRIL 2011**

**SYNTHESIS AND CHARACTERIZATION OF METAL TELLURIDES AND
ANTIMONIDES FOR USING AS THERMOELECTRIC MATERIALS**

TAWAT SURIWONG

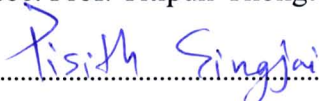
THIS THESIS HAS BEEN APPROVED
TO BE A PARTIAL FULFILLMENT OF THE REQUIREMENTS
FOR THE DEGREE OF DOCTOR OF PHILOSOPHY
IN MATERIALS SCIENCE

EXAMINING COMMITTEE

..... CHAIRPERSON
Assoc. Prof. Dr. Vittaya Amornkitbamrung

..... MEMBER
Prof. Dr. Somchai Thongtem

..... MEMBER
Assoc. Prof. Titipun Thongtem

..... MEMBER
Assoc. Prof. Dr. Pisith Singjai

..... MEMBER
Assoc. Prof. Dr. Dheerawan Boonyawan

THESIS ADVISORY COMMITTEE

..... ADVISOR
Prof. Dr. Somchai Thongtem

..... CO-ADVISOR
Assoc. Prof. Titipun Thongtem

..... CO-ADVISOR
Assoc. Prof. Dr. Pisith Singjai

29 April 2010

© Copyright by Chiang Mai University

ACKNOWLEDGEMENTS

First, I would like to thank Prof. Dr. Somchai Thongtem, my supervisor, for great opportunities, guidance, supervisions, valuable suggestions and all supports throughout my Ph.D study. Second, I would like to give a special thank to the committee, Assoc. Prof. Titipun Thongtem, Assoc. Prof. Dr. Pisith Singjai, Asst. Prof. Dr. Supab Choopun, and Assoc. Prof. Dr. Dheerawan Boonyawan for all kind advices, helpful suggestions and valuable information of this thesis, including Assoc. Prof. Dr. Vittaya Amornkitbamrung, external committee as the chairperson. I have learned an incredible amount during my three years of stusy. Most importantly I am very grateful to be a good scientist.

I am very grateful the Thailand Research Fund (TRF), Bangkok, Thailand for awarding the scholarship through the Royal Golden Jubilee Ph.D. program (RGJ-Ph.D.). I would like to express my deep appreciation to Prof. Dr. Shinsuke Yamanaka, and Assoc. Prof. Dr. Ken Kurosaki for the opportunity and important knowledge of thermoelectric materials while I was a research fellow at the Future Resource, Energy, and Eco materials (FREE) Research Unit, Graduate School of Engineering, Osaka University, Japan.

I would like to thank all helps and supports of secretaries and technical staffs of the Department of Physics and Materials Science, Department of Chemistry, and Electron Microscopy Research and Service Center, Faculty of Science, Chiang Mai University. Many thanks to my classmates, lab members and friends for their help, support and cheer.

Finally, I would like to give thank Mr. Prachuap Suriwong and Mrs. Sane Suriwong, my parents, my brother and sister and Ms. Voraluck Thongbor for their love, kindness, support and encourage me at all time.

Tawat Suriwong

Thesis Title	Synthesis and Characterization of Metal Tellurides and Antimonides for Using as Thermoelectric Materials	
Author	Mr. Tawat Suriwong	
Degree	Doctor of Philosophy (Materials Science)	
Thesis Advisory Committee	Prof. Dr. Somchai Thongtem	Advisor
	Assoc. Prof. Titipun Thongtem	Co-Advisor
	Assoc. Prof. Dr. Pisith Singjai	Co-Advisor

ABSTRACT

E 47207

In this research, thermoelectric materials: ZnTe and Sb₂Te₃ were successfully synthesized by microwave heating and microwave generating of plasma for solid-state reaction. Cubic ZnTe nanocrystals were synthesized from 1:1, 1.5:1 and 1.8:1 molar ratios of Zn:Te by a 900 W microwave plasma. Their green emissions were detected at 562 nm (2.21 eV) using luminescence spectrophotometry. Sb₂Te₃ with a rhombohedral crystal system was successfully synthesized by an environmentally benign process with a short reaction time using a 900 W irradiated microwave plasma. At 2:2, 2:1.75, and 2:1.5 molar ratios of Sb:Te, with time lengths of 10 and 20 min,

the products were pure Sb_2Te_3 phase with no detection of any residues. The direct energy gaps were determined to be 0.340–0.515 eV.

In addition, Ni_3GaSb and Ni_3InSb were successfully synthesized by alloying synthesis at high temperature in closed silica ampoules. Ni_3GaSb and Ni_3InSb compounds indicated metal-like characteristics in α and ρ . The power factor ($\alpha^2\rho^{-1}$) values increased with temperature and reached maximum at 1073 K. The thermal conductivity (κ) and dimensionless figure of merit ZT of both samples were increased with temperature as well. The maximum values of the ZT for Ni_3GaSb and Ni_3InSb at 1073 K were achieved to be 0.022 and 0.023, respectively.

ชื่อเรื่องวิทยานิพนธ์	การสังเคราะห์และการหาลักษณะเฉพาะของโลหะเทลลูไรด์และแอนติโมนิไนด์สำหรับใช้เป็นวัสดุเทอร์โมอิเล็กทริก	
ผู้เขียน	นายธวัช สุริวงษ์	
ปริญญา	วิทยาศาสตร์ดุขฎิบัณชิต (วัสดุศาสตร์)	
คณะกรรมการที่ปรึกษาวิทยานิพนธ์	ศ. ดร. สมชาย ทองเต็ม	อาจารย์ที่ปรึกษาหลัก
	รศ. ธิติพันธุ์ ทองเต็ม	อาจารย์ที่ปรึกษาร่วม
	รศ. ดร. พิศิษฐ์ สิงห์ใจ	อาจารย์ที่ปรึกษาร่วม

บทคัดย่อ

E 47207

งานวิจัยนี้ เป็นการสังเคราะห์วัสดุเทอร์โมอิเล็กทริก คือ ZnTe และ Sb_2Te_3 ด้วยวิธีพลาสมาของรังสีไมโครเวฟเพื่อให้เกิดปฏิกิริยาของของแข็ง ซึ่งประสบความสำเร็จในการสังเคราะห์ ZnTe ที่มีขนาดผลึกในระดับนาโนเมตร ด้วยอัตราส่วนโดยโมลของ Zn:Te เท่ากับ 1:1, 1.5:1 และ 1.8:1 ที่ 900 W ไมโครเวฟ โดยสาร ZnTe นี้เรืองแสงสีเขียวที่มีความยาวคลื่น 562 nm (2.21 eV) สำหรับการสังเคราะห์สาร Sb_2Te_3 มีการใช้ 900 W ไมโครเวฟ ที่อัตราส่วนโดยโมลของ Sb:Te เท่ากับ 2:2, 2:1.75 และ 2:1.5 และเวลาในการทำปฏิกิริยาเป็น 10 และ 20 นาที ตามสภาวะการทดลองนี้ทำให้สังเคราะห์สาร Sb_2Te_3 มีความบริสุทธิ์เมื่อทำการวิเคราะห์หาช่องว่างพลังงานพบว่าอยู่ในช่วง 0.340-0.515 eV

นอกจากนี้ยังได้สังเคราะห์สารประกอบ Ni_3GaSb และ Ni_3InSb ให้เกิดปฏิกิริยาในหลอดสุญญากาศที่ปิดสนิทที่อุณหภูมิสูง ผลการทดลองของสารประกอบ Ni_3GaSb และ Ni_3InSb พบว่ามีค่า α และ ρ ที่มีสมบัติคล้ายโลหะ โดยค่า power factor และ dimensionless figure of merit มีค่าเพิ่มขึ้นเมื่ออุณหภูมิสูงขึ้น และมีค่าสูงสุดที่ 1073 K โดย dimensionless figure of merit ของ Ni_3GaSb และ Ni_3InSb มีค่าเท่ากับ 0.022 และ 0.023 ตามลำดับ

TABLE OF CONTENTS

	Page
ACKNOWLEDGEMENTS	iii
ABSTRACT (ENGLISH)	v
ABSTRACT (THAI)	vii
LIST OF TABLES	xii
LIST OF FIGURES	xiv
LIST OF APPENDIX TABLES	xx
LIST OF APPENDIX FIGURES	xxi
ABBREVIATIONS AND SYMBOLS	xxii
CHAPTER 1 INTRODUCTION	1
Research objective	6
CHAPTER 2 LITERATURE REVIEW	7
2.1 Thermoelectric materials	7
2.1.1 Principles of thermoelectric energy conversion	7
2.1.2 Definition and description of the figure of merit	10
2.1.3 Conflicting thermoelectric material properties	11
2.1.4 Thermoelectric modules: devices	20
2.1.5 Thermoelectric efficiency	24
2.2 Microwave irradiation/heating	25
2.2.1 Dielectric heating	25

2.2.2 Microwave plasma	28
2.3 Solid-state reaction	35
2.3.1 General aspects of solid-state reactions	36
2.3.2 Formation of metastable solids	39
2.4 Synthesis/alloying preparation	40
2.5 Sintering	42
2.5.1 Stages of sintering	44
2.5.2 Factors affecting sintering	46
2.5.3 Spark-plasma sintering	47
2.6 ZnTe	48
2.6.1 Structure	48
2.6.2 Applications	50
2.6.3 Synthesis of ZnTe	52
2.7 Sb ₂ Te ₃	57
2.7.1 Structure	57
2.7.3 Synthesis of Sb ₂ Te ₃	60
2.8 Ni ₃ GaSb and Ni ₃ InSb	64
CHAPTER 3 EXPERIMENTAL PROCEDURE	66
3.1 Chemical reagents, and instruments	66
3.1.1 Chemical reagents	66
3.1.2 Instruments	66
3.2 Synthesized methods	67
3.2.1 Synthesis of ZnTe using microwave plasma	67

3.2.2	Synthesis of Sb_2Te_3 using microwave plasma	68
3.2.3	Synthesis of Ni_3GaSb and Ni_3InSb using alloying preparation in a furnace	69
3.3	Characterization	71
3.3.1	X-ray diffraction (XRD)	71
3.3.2	Scanning electron microscope (SEM) and energy dispersive X-ray analyser	72
3.3.3	Transmission electron microscope (TEM)	74
3.3.4	Luminescence spectrometer	74
3.3.5	UV-Vis-NIR spectrophotometer	74
3.3.6	Raman spectrometer	76
3.3.7	Seebeck coefficient/electric resistance measuring system	77
3.3.8	Hall effect measurement system	78
3.3.10	Laser flash thermal constants analyzer	80
CHAPTER 4	RESULTS AND DISCUSSION	81
4.1	ZnTe by microwave plasma	81
4.2	Sb_2Te_3 by microwave plasma	102
4.3	Ni_3GaSb and Ni_3InSb by alloying preparation in a furnace	109
CHAPTER 5	CONCLUSIONS AND SUGGESTIONS	119
5.1	ZnTe by microwave plasma	119
5.2	Sb_2Te_3 by microwave plasma	119
5.3	Ni_3GaSb and Ni_3InSb by alloying preparation in a furnace	120

5.4 Suggestions	120
REFERENCES	122
APPENDICES	133
APPENDIX A The Joint Committee for Powder Diffraction Standards (JCPDS)	134
APPENDIX B Camera constant used for the indexing of SAED pattern	150
APPENDIX C Microwave induced plasma system	151
APPENDIX D The results of the Rietveld refinement analysis	152
APPENDIX E International Publications	156
CURRICULUM VITAE	169

LIST OF TABLES

Table	Page	
2.1	Microwave active elements, natural minerals, and compounds	29
2.2	Melting temperatures and total vapor pressures of major thermoelectric materials	40
2.3	The property and structure of ZnTe	50
2.4	Lengths of bond and angles between them in Sb ₂ Te ₃	59
4.1	Calculated lattice parameter of ZnTe from the experiment (molar ratio of Zn:Te = 1:1, 40 min.) comparing with the JCPDS file (Reference code: 15-0746 for ZnTe)	83
4.2	Calculated lattice parameter of ZnTe from the experiment (molar ratio of Zn:Te = 1.5:1, 40 min.) comparing with the JCPDS file (Reference codes: 15-0746 for ZnTe)	85
4.3	Calculated lattice parameter of ZnTe from the experiment (molar ratio of Zn:Te = 1.8:1, 20 min.) comparing with the JCPDS file (Reference codes: 15-0746 for ZnTe)	87
4.4	The 2 θ diffraction angles and intensities of the JCPDS no. 15-0746 and for the 1:1 molar ratio of Zn:Te and 40 min product obtained from the experiment and simulation	88

4.5	The 2θ diffraction angles and intensities of the JCPDS no. 15-0746 and for the 1.5:1 molar ratio of Zn:Te and 40 min product obtained from the experiment and simulation	88
4.6	The 2θ diffraction angles and intensities of the JCPDS no. 15-0746 and for the 1.8:1 molar ratio of Zn:Te and 20 min. product obtained from the experiment and simulation	89
4.7	The crystallite size (D) calculated from the Scherrer's equation and the full-width at half maximum (FWHM) of the XRD spectra	90
4.8	Ring diffraction pattern values of ZnTe produced under the 1:1 molar ratio of Zn:Te condition	96
4.9	Ring diffraction pattern values of ZnTe produced under the 1.5:1 molar ratio of Zn:Te condition	97
4.10	Ring diffraction pattern values of ZnTe produced under the 1.8:1 molar ratio of Zn:Te condition	98
4.11	Crystallite sizes of Sb_2Te_3 crystals synthesized at different Sb:Te molar ratios and lengths of time by 900 W microwave plasma	104
4.12	Direct energy band gaps of Sb_2Te_3 crystals synthesized at different Sb:Te molar ratios and lengths of time by 900 W microwave plasma	109
4.13	Lattice parameters, sample bulk density, and chemical composition of Ni_3GaSb and Ni_3InSb	113
4.14	Hall coefficient (R_H), Hall carrier concentration (n_H) and Hall Mobility (μ_H) at 300 K	117

LIST OF FIGURES

Figure		Page
2.1	Thermodynamic circuit for the relative Seebeck coefficient	8
2.2	Schematic diagram of thermoelectric power generation	9
2.3	Thermodynamic circuit for the Peltier effect	10
2.4	Schematic diagram of thermoelectric refrigeration	10
2.5	Optimizing ZT through carrier concentration tuning	13
2.6	Complex crystal structures that yield low lattice thermal conductivity. Extremely low thermal conductivities are found in the recently identified complex material systems	16
2.7	Reducing the lattice thermal conductivity leads to a two-fold benefit for the thermoelectric figure of merit	18
2.8	TE heat engines. (A) When current is run across a TE junction, it heats or cools through the Peltier effect, depending on the direction of the current flow. (B) When heat flows across the junction, electrical current is generated through the Seebeck effect. (C) Practical TE generators connect large numbers of junctions in series to increase operating voltage and spread heat flow	21
2.9	Thermoelectric module showing the direction of charge flow on both cooling and power generation	22

2.10	Dimensionless Figure of merit ZT shown as a function of temperature for several bulk thermoelectric materials	23
2.11	Dipole rotations of molecule occurs in materials containing polar molecules having an electrical dipole moment, which will align molecules in a microwave electromagnetic field	26
2.12	Molecular rotation which energy in the form of microwave electromagnetic radiation	27
2.13	Schematic diagram of Cober microwave system used in the synthesis of binary nitride materials by exposing in a nitrogen plasma	30
2.14	Schematic diagram of (a) the apparatus for plasma modification by making use of an atmospheric microwave plasma torch, and (b) the construction of the plasma nozzles	32
2.15	A photograph of the microwave plasma in operation for the treatment of Al sample	33
2.16	Schematic presentation of the synthetic system of MgO nanoparticles with the atmospheric microwave plasma torch. The inset shows the plasma emission of green color after completion of the synthesis	33
2.17	A schematic diagram of microwave plasma equipment	34
2.18	Reaction of two crystals (A and B) sharing one face. After initial formation of a product layer C, ions from A and B have to counter-diffuse through the product layer to form new product at the A/C and B/C interfaces	36

2.19	The relation of thickness and time for $n = 1$, and 3. The curve for $n = 3$ graphically shows the induction period at the beginning of the reaction	38
2.20	Synthesis/alloying ampoule preparation	41
2.21	Diffusion of different paths during sintering	43
2.22	A two-dimensional sphere model, illustrating the first two stages during sintering	45
2.23	(a) Spark Plasma sintering system, and (b) graphite die during the SPS operation.	47
2.24	ZnTe single crystal	49
2.25	The ZnTe structure (a) zinc blende (cubic) and (b) wurtzite	49
2.26	The ZnTe applications (a) semiconductor diodes, (b) electro-optics, (c) solar cells, (d) assorted discrete transistors and (e) light-emitting diodes (LED)	51
2.27	Crystal structure of the thermoelectric Sb_2Te_3 materials. The blue atoms are Sb and the pink atoms are Te	58
2.28	Dimensionless figure of merit ZT of commercial materials and those used or being developed by NASA for thermoelectric power generation. (a) n -type and (b) p -type	60
2.29	(a) Unit cell of the $\text{B8}_{1.5}$ structure, (b) Unit cell of the $\text{B8}_{1.5}$ structure as viewed along the c -axis	65
3.1	Schematic diagram of microwave induced plasma system	68
3.2	Spark plasma sintering machine, model SPS-515A, Syntex, Japan	71

3.3	X-ray diffractometer	72
3.4	(a) Field emission-scanning electron microscope and (b) Scanning electron microscope	73
3.5	Transmission electron microscope	73
3.6	Luminescence spectrometer	74
3.7	UV-Vis-NIR Spectrophotometer	75
3.8	Raman spectrometer	76
3.9	Seebeck Coefficient/Electric Resistance Measuring System	77
3.10	Schematic of a van der Pauw configuration used for the determination of Hall voltage V_H	79
3.11	Hall effect measurement system	79
3.12	Laser Flash Thermal Constants Analyzer	80
4.1	XRD spectra of the products prepared using 1:1 molar ratio of Zn:Te	82
4.2	XRD spectra of the products prepared using 1.5:1 molar ratio of Zn:Te	84
4.3	XRD spectra of the products prepared using 1.8:1 molar ratio of Zn:Te	86
4.4	XRD spectra simulation of ZnTe at (a) 1:1, (b) 1.5:1 and (c) 1.8:1 molar ratio of Zn:Te	89
4.5	Raman spectra of ZnTe synthesized using 1:1 molar ratio of Zn:Te for 40 min	91
4.6	SEM image and particle size distribution of ZnTe produced under the 1:1 molar ratio of Zn:Te for 40 min condition	92

4.7	SEM image and particle size distribution of ZnTe produced under the 1.5:1 molar ratio of Zn:Te for 40 min condition	93
4.8	SEM image and particle size distribution of ZnTe produced under the 1.8:1 molar ratio of Zn:Te for 20 min condition	94
4.9	TEM image (a) and SAED patterns (b) of ZnTe produced under the 1:1 molar ratio of Zn:Te condition	96
4.10	TEM image (a) and SAED patterns (b) of ZnTe produced under the 1.5:1 molar ratio of Zn:Te condition	97
4.11	TEM image (a) and SAED patterns (b) of ZnTe produced under the 1.8:1 molar ratio of Zn:Te condition	98
4.12	Photoluminescence of ZnTe produced under the 1:1 molar ratio of Zn:Te condition	100
4.13	Photoluminescence of ZnTe produced under the 1.5:1 molar ratio of Zn:Te condition	100
4.14	Photoluminescence of ZnTe produced under the 1.8:1 molar ratio of Zn:Te condition	101
4.15	XRD spectra of the products synthesized using 900 W microwave plasma at different molar ratios of Sb:Te for 10 min and 20 min	103
4.16	Raman spectra of Sb ₂ Te ₃ synthesized using 900 W microwave plasma for different molar ratios of Sb:Te and lengths of time	105
4.17	SAED patterns, and SEM and HRTEM images of Sb ₂ Te ₃ synthesized using 900 W microwave plasma for different molar ratios of Sb:Te and lengths of time. (a) 2:1.5, 10 min; (b, c) 2:1.5, 20 min; and (d - f)	106

	2:2, 20 min.	
4.18	The $(\alpha_{abs}hv)^2$ vs (hv) plots of Sb_2Te_3 , synthesized at different Sb:Te molar ratios and lengths of time by 900 W microwave plasma	108
4.19	Powder XRD patterns of the polycrystalline samples; (a) Ni_3GaSb and (b) Ni_3InSb , including their databases (c) and (d)	110
4.20	Powder XRD patterns of the polycrystalline samples and the results of the Rietveld refinement of (a) Ni_3GaSb and (b) Ni_3InSb . The experimental data are labelled as small red crosses, the calculated fits and the difference curves are shown as blue solid lines. Short vertical lines (green) below the patterns indicate the calculated peak positions	111
4.21	Crystal structures of Ni_3GaSb and Ni_3InSb	112
4.22	SEM and EDX mapping images of the (a) Ni_3GaSb and (b) Ni_3InSb bulk samples	114
4.23	Temperature dependences of the electrical properties of Ni_3GaSb and Ni_3InSb polycrystalline samples: (a) electrical resistivity ρ , (b) Seebeck coefficient α , and (c) power factor $\alpha^2\rho^{-1}$	116
4.24	Temperature dependences of the (a) thermal conductivity κ and (b) dimensionless Figure of merit ZT of Ni_3GaSb and Ni_3InSb polycrystalline samples	117

LIST OF APPENDIX TABLE

Table		Page
B1	TEM constant ($L\lambda$) at 200 kV	150

LIST OF APPENDIX FIGURES

Figure		Page
C1	Microwave induced plasma system	151
C2	Microwave induced plasma system during operation	151

ABBREVIATIONS AND SYMBOLS

RF	=	Radio frequency
kW	=	Kilowatts
AC	=	Alternating current
DC	=	Direct current
°C	=	Degree celcius
cm	=	Centimeter
mm	=	Millimeter
μm	=	Micrometer
nm	=	Nanometer
Å	=	Angstrom
EDX	=	Energy dispersive X-ray spectroscopy
FT-IR	=	Fourier-transform infrared spectrometry
PL	=	Photoluminescence spectrometry
SEM	=	Scanning electron microscopy
TEM	=	Transmission electron microscopy
XRD	=	X-ray diffraction spectrometer
JCPDS	=	The Joint Committee for Powder Diffraction Standards
SPS	=	Spark plasma sintering
Z	=	Figure of merit
ZT	=	Dimensionless figure of merit
TE	=	Thermoelectric

C_p	=	Heat capacity
D	=	Crystallite size
K	=	Geometric (shaped) factor
E_{el}	=	The electric field strength
E_g	=	Energy band gap
N	=	Number of atoms in the unit cell
R	=	Gas constant
T	=	Temperature
T_H	=	Hot-site temperature
T_C	=	Cold-site temperature
V	=	Unit cell volume
b	=	The path length
α	=	Seebeck coefficients
ρ	=	Electrical resistivity
σ	=	Electrical conductivity
κ	=	Thermal conductivity
κ_{lat}	=	Lattice thermal conductivity
κ_{el}	=	Electronic thermal conductivity
κ_{dif}	=	Thermal diffusivity
α_{abs}	=	Total absorption coefficient
k_B	=	Boltzmann constant
k	=	The rate constant of reaction
h	=	Planck's constant

t	=	Time
x	=	The amount of reaction
ν	=	Photon frequency
d	=	Interplanar planes
d	=	Sample density
d_{th}	=	Theoretical density
d_{exp}	=	Measured density
$d_{\text{exp}/d_{\text{exp}}}$	=	Relative density
n_s	=	Sheet carrier density
n_H	=	Hall carrier concentration
V_H	=	Hall voltage
I	=	Current
B	=	Constant magnetic field
q	=	Elementary charge
R_H	=	Hall coefficient
μ_H	=	Hall mobility
Φ	=	Coefficient of performance
η	=	Efficiency
W	=	Power input
Q_H	=	Net heat flow rate
ω	=	Angular frequency
ε_r''	=	The imaginary part of the complex relative permittivity
ε_0	=	The permittivity of free space